Eur. Phys. J. D (2013) 67: 3
DOI: 10.1140/epjd/e2012-30423-7

THE EUROPEAN PHYSICAL JOURNAL D

Regular Article

Density functional study of geometrical, electronic and magnetic properties of W_n clusters (n = 2–16, 19, 23)

Samanta M. Carrión[1], Reinaldo Pis-Diez[1,a], and Faustino Aguilera-Granja[2]

[1] CEQUINOR, Centro de Química Inorgánica (CONICET, UNLP), Departamento de Química, Facultad de Ciencias Exactas, UNLP, C.C. 962, 1900 La Plata, Argentina
[2] Instituto de Física "Manuel Sandoval Vallarta", Universidad Autónoma de San Luis Potosí, 78000 S.L.P., México

Received 6 July 2012 / Received in final form 14 October 2012
Published online 24 January 2013 – © EDP Sciences, Società Italiana di Fisica, Springer-Verlag 2013

Abstract. Geometrical, electronic and magnetic properties of W_n atomic clusters, with $n = 1$–16, 19, 23, are explored using different generalized gradient approximations to the density functional theory and basis sets of double-ζ quality augmented with polarization functions. From a geometrical point of view, tungsten aggregates with $n = 15$ and above exhibit a clear tendency to adopt structures derived from the body-centered cubic system. Total energy second-differences indicate that tungsten octamer becomes a specially stable isomer. For larger sizes, the different generalized gradient approximations do not predict the same stability pattern. Vertical ionization energies show a smooth, but slow trend to the experimental work function of polycrystalline tungsten. Vertical electron affinities agree very well with experimental measures of detachment electron energies. Calculated magnetic moments indicate that mainly singlet, triplet and quintet electronic states characterize small tungsten aggregates. A W_{15} isomer with a geometry derived from the body-centered cubic system, however, is characterized by an electronic state with 14 unpaired electrons.

1 Introduction

Transition metals are between the most widely used systems in heterogeneous catalysis. Tungsten compounds, particularly in the form of oxides and sulfides, are the basis of a series of catalysts used in a variety of important chemical processes, such as hydrocracking and hydrotreating [1].

Nanoclusters are aggregates that can present from a few to many millions of atoms or molecules. The continuous interest in nanocluster science arises because these aggregates are a new type of material, whose properties differ both from those of isolated atoms or molecules and from those of bulk materials. Interestingly, those unique properties can be studied in different media such as the vapor phase or on surfaces [2]. For this reason, transition metal clusters, both free and supported, constitute an exciting alternative to the classical catalysts [3].

The chemical reactivity of small tungsten clusters up to 60 atoms with dinitrogen was studied experimentally at different temperatures [4,5]. It is reported in those works that tungsten clusters, W_n, change their reactivity pattern at $n = 15$, suggesting that a structural transition from closed-packed forms to more open structures takes place. Another experimental study on the interaction of atomic nitrogen and dinitrogen with anionic tungsten aggregates up to the octamer revealed that chemisorption of N_2 is preferred to dissociation [6].

On the theoretical side, previous works were restricted to neutral and charged tungsten clusters of less than six atoms [7–9]. Very recently, however, a systematic density functional theory study on W_n clusters, with $n = 2$–16, was accomplished using the BPW91 generalized gradient approximation (GGA) to the density functional theory (DFT) and a set of numerical basis functions of double-ζ quality augmented with polarization functions [10]. The authors found that larger W clusters show structures that can be considered as derivatives of the body-centered cubic structure of bulk tungsten. Moreover, they predict that aggregates with 8, 12 and 15 atoms should be more stable than their immediate neighbors.

In the present work, geometric, electronic and magnetic properties of small tungsten clusters W_n, with $n = 2$–16, 19, 23, are studied within the framework of the DFT, using two different codes to offer a wider perspective on the features of those transition-metal clusters. Special emphasis is laid on the magnetic moments of the aggregates and the suggested structural transition at $n = 15$. The two highest sizes, $n = 19$ and $n = 23$ are added to the present study because they are related to symmetric body-centered cubic structures, and bulk tungsten adopts the same body-centered cubic structure.

[a] e-mail: pis_diez@quimica.unlp.edu.ar

2 Computational details

To investigate the geometrical structure and the electronic and magnetic properties of free-standing W_n aggregates, with n = 2–16, 19, 23, two different codes are used. Although both are based on the DFT [11–13], they differ on the way in which atomic states are mathematically modeled.

The first program, the SIESTA package [14], uses numerical pseudoatomic orbitals as basis sets to solve the single particle Kohn-Sham equations. The Perdew-Burke-Ernzerhof gradient-corrected functional [15] is used to model exchange-correlation effects. Atomic cores are described by a nonlocal, norm-conserving Troullier-Martins pseudopotential [16] factorized in the Kleinman-Bylander form [17]. The pseudopotential for W is generated using the $5d^4\ 6s^2\ 6p^0$ valence configuration with cutoff radii of 2.24, 2.85, 3.03 a.u. for the d, s and p states, respectively. Core corrections are included using a radius of 1.30 a.u. Valence states are described by a double-ζ basis set, which is augmented by two sets of polarization functions. Thus, this method will be referred to as PBE/DZP. Calculations are carried out in a supercell of size $20 \times 20 \times 20$ Å^3, which is large enough to avoid interactions with neighbor cells. Moreover, such a box size allows to consider only the Γ point ($k = 0$) when integrating over the Brillouin zone. The energy cutoff used to define the real-space grid for the numerical calculations involving the electron density is 250 Ry. Geometry optimizations are performed without symmetry constrains until interatomic forces are smaller than 0.006 eV/Å. No constrains are imposed to the electronic spin multiplicity during geometry optimizations.

The second program used in the present work is the Amsterdam density functional (ADF) code [18–20], which uses Slater-type functions to model atomic orbitals instead of the usual Gaussian-type functions. The gradient-corrected functional due to Becke is used to model exchange effects [21], whereas electron correlation is accounted for via the functional developed by Lee et al. [22]. A double-ζ basis set of Slater-type functions including a set of polarization functions is used throughout. Thus, this method will be referred to as BLYP/DZP. The frozen core approximation up to the $4d$ orbital (included) is utilized. Relativistic effects are taken into account through the zero order regular approximation (ZORA) [23–25]. No symmetry constrains are imposed during geometry optimizations. In the case of the ADF program, both the geometry of the cluster and its electronic spin multiplicity are considered as variables in the total electronic energy minimization. Geometries are considered optimized when the interatomic forces are below a threshold of 0.005 eV/Å.

A variety of atomic configurations are considered as starting points for geometry optimization. Those configurations are chosen according to: (i) compact structures based on close-packed units such as body-centered and face-centered cubic systems, generally presented in $3d$-transition metal clusters; (ii) open structures based on the simple cubic motif as observed in $4d$ and $5d$ transition metal clusters; (iii) structures designed by adding a single atom to the lowest energy structures with $N-1$ atoms; (iv) atomic structures reported in the literature for previous calculations on clusters having similar sizes and formed by elements, which are close in the periodic table.

Table 1. Energy difference, in eV, between the two lowest atomic states of neutral W calculated with different DFT levels of theory using ADF. The experimental difference is also shown. Value in parenthesis under column PBE was obtained with SIESTA at the level of theory indicated in text.

Atomic state	Exp.[26]	BPW91	PBE	BLYP
$d^4\ s^2\ (^5\mathrm{D})$	0.0	0.0	0.0	0.0
$d^5\ s^1\ (^7\mathrm{S})$	0.3695	–0.8800	–0.8669	–0.2200
			(–0.7284)	

The atomization energy of a given W_n aggregate is calculated as $E_{at} = E(\mathrm{W}) - E(\mathrm{W}_n)/n$, where $E(\mathrm{W})$ is the energy of the ^{7}S atomic state of W, which corresponds to the [Xe] $f^{14}\ d^5\ s^1$ electronic configuration. It is important to stress here that although the ground state of atomic W is known to be a ^{5}D atomic state corresponding to the [Xe] $f^{14}\ d^4\ s^2$ electronic configuration [26], DFT calculations predict the ^{7}S atomic state to be the ground state. This is exemplified in Table 1. Due to this fact, all atomization energies reported in the present work use the ^{7}S atomic state as reference.

As a measure of the relative stability of clusters of different sizes, the second-order total energy difference is calculated according to $\Delta_2 E(n) = E(\mathrm{W}_{n+1}) + E(\mathrm{W}_{n-1}) - 2E(\mathrm{W}_n)$.

Vertical ionization energies (VIE) and vertical electron affinities (VEA) are calculated as $VIE(n) = E(\mathrm{W}_n^+) - E(\mathrm{W}_n)$ and $VEA(n) = E(\mathrm{W}_n) - E(\mathrm{W}_n^-)$, respectively. The geometries of ionized aggregates are those of the corresponding neutral clusters. When neutral clusters exhibit an open shell electronic configuration, different electron multiplicities are considered for ionized species as a variable for minimizing the total electronic energy.

An arbitrary threshold of 3.20 Å is considered to calculate average bond lengths between neighbors and average coordination numbers. That threshold corresponds to about 20% in excess to the W-W bond distance in bulk tungsten.

3 Results and discussion

3.1 Geometrical features of W_n clusters

It is important to clarify that although several stable structures are found for different sizes, only the two more stable aggregates for each size are reported as the interest is mainly focused on the evolution of electronic properties and magnetic moments with size, and the eventual structural transition at $n = 15$. Exceptions are $n = 6$, $n = 19$ and $n = 23$, for which ADF allows to obtain a ground state

Table 2. Atomization energies, E_{at} in eV/at, average bond lengths, R_{av} in Å, average coordination numbers, CN, and magnetic moments, μ in μ_B, for W_n clusters, with $n = 2$–7. See Figures 1 and 2 for labels.

Size	Method	E_{at}	R_{av}	CN	μ
2	SIESTA	2.60	1.835	1.00	0.00
	ADF	2.69	2.076	1.00	0.00
	Reference [10]	2.61	2.053	1.0	0.00
3	SIESTA - *a*	3.15	2.235	2.00	0.67
	SIESTA - *b*	3.05	2.236	2.00	0.00
	ADF - *a*	3.37	2.348	2.00	0.67
	ADF - *b*	3.33	2.365	2.00	0.00
	Reference [10]	3.63	2.327	2.0	–
4	SIESTA - *a*	3.59	2.509	3.00	0.00
	SIESTA - *b*	3.54	2.360	2.50	0.50
	ADF - *a*	3.90	2.611	3.00	0.00
	ADF - *b*	3.78	2.528	3.00	0.50
	Reference [10] - *a*	4.12	2.468	3.0	–
	Reference [10] - *b*	4.11	2.306	2.0	–
	Reference [10] - *c*	4.10	2.445	3.0	–
	Reference [10] - *d*	4.06	2.444	3.0	–
5	SIESTA - *a*	4.02	2.516	3.60	0.40
	SIESTA - *b*	4.00	2.517	3.60	0.00
	ADF - *a*	4.28	2.602	3.60	0.40
	ADF - *b*	4.06	2.546	3.20	0.80
	Reference [10] - *a*	4.61	2.438	2.8	–
	Reference [10] - *b*	4.39	2.429	2.4	–
	Reference [10] - *c*	4.05	2.384	2.4	–
6	SIESTA - *a*	4.31	2.556	4.00	0.33
	SIESTA - *b*	4.23	2.528	4.00	0.00
	ADF	4.57	2.630	4.00	0.33
	Reference [10] - *a*	4.91	2.533	4.0	–
	Reference [10] - *b*	4.81	2.552	4.0	–
	Reference [10] - *c*	4.77	2.563	4.0	–
7	SIESTA - *a*	4.48	2.560	4.29	0.29
	SIESTA - *b*	4.43	2.546	4.29	0.00
	ADF - *a*	4.73	2.635	4.29	0.29
	ADF - *b*	4.73	2.625	4.29	0.29
	Reference [10] - *a*	5.13	2.573	4.0	–
	Reference [10] - *b*	5.04	2.574	4.3	–
	Reference [10] - *c*	4.99	2.575	4.3	–

Table 3. Atomization energies, E_{at} in eV/at, average bond lengths, R_{av} in Å, average coordination numbers, CN, and magnetic moments, μ in μ_B, for W_n clusters, with $n = 8$–12. See Figures 1, 2, 3 and 4 for labels.

Size	Method	E_{at}	R_{av}	CN	μ
8	SIESTA - *a*	4.69	2.587	4.50	0.50
	SIESTA - *b*	4.68	2.578	4.50	0.25
	ADF - *a*	4.90	2.652	4.50	0.25
	ADF - *b*	4.90	2.661	4.50	0.50
	Reference [10] - *a*	5.31	2.601	4.5	–
	Reference [10] - *b*	5.28	2.593	4.5	–
	Reference [10] - *c*	5.21	2.503	3.0	–
	Reference [10] - *d*	5.16	2.519	4.0	–
	Reference [10] - *e*	5.13	2.583	4.5	–
9	SIESTA - *a*	4.75	2.550	4.44	0.00
	SIESTA - *b*	4.75	2.550	4.44	0.22
	ADF	4.98	2.642	4.67	0.00
	Reference [10] - *a*	5.36	2.590	4.7	–
	Reference [10] - *b*	5.32	2.621	4.7	–
	Reference [10] - *c*	5.29	2.637	4.7	–
10	SIESTA - *a*	4.86	2.598	4.80	0.60
	SIESTA - *b*	4.84	2.605	5.00	0.20
	ADF - *a*	5.07	2.663	5.00	0.20
	ADF - *b*	5.03	2.664	4.80	0.40
	Reference [10] - *a*	5.44	2.613	4.8	–
	Reference [10] - *b*	5.42	2.600	4.6	–
	Reference [10] - *c*	5.42	2.621	4.8	–
11	SIESTA - *a*	4.92	2.608	5.09	0.00
	SIESTA - *b*	4.91	2.618	4.91	0.36
	ADF - *a*	5.20	2.661	5.09	0.18
	ADF - *b*	5.10	2.680	4.91	0.18
	Reference [10] - *a*	5.51	2.650	5.3	–
	Reference [10] - *b*	5.51	2.670	5.5	–
	Reference [10] - *c*	5.42	2.627	4.5	–
12	SIESTA - *a*	4.97	2.611	5.17	0.00
	SIESTA - *b*	4.97	2.614	5.00	0.17
	ADF - *a*	5.19	2.667	5.17	0.00
	ADF - *b*	5.19	2.671	5.00	0.00
	Reference [10] - *a*	5.63	2.604	5.0	–
	Reference [10] - *b*	5.58	2.601	5.0	–
	Reference [10] - *c*	5.57	2.718	6.0	–
	Reference [10] - *d*	5.45	2.625	5.0	–

that is well separated from other stable structures. Thus, in those cases only the most stable isomer is reported.

Atomization energies, average bond lengths, average coordination numbers and magnetic moments are listed in Tables 2, 3 and 4 for sizes $n = 2$ to $n = 7$, $n = 8$ to $n = 12$ and $n = 13$ to $n = 23$, respectively. Figures 1 to 6 show the equilibrium geometries of W_n aggregates from $n = 4$ to $n = 23$ as obtained with the two programs used in the present work.

The dimer is used to test the validity of the methodologies used throughout. It can be seen from Table 2 that all methods predict a singlet electronic state as the ground state for W_2, with atomization energies ranging from 2.60 to 2.69 eV/at. This is in agreement with the experimental value of 5 ± 1 eV [27]. The bond distance calculated with ADF is in good agreement with other calculated values. SIESTA, on the other hand, provides a shorter bond distance.

Both SIESTA and ADF predict an equilateral triangle characterized by a triplet electronic state to be the ground state of W_3. This is in agreement with the geometry and electronic state reported in reference [10]. ADF also predicts an isosceles triangle being only 0.04 eV/at above the ground state, whereas SIESTA allows to find another equilateral triangle 0.10 eV/at above the ground state. In both cases, a singlet electronic state characterizes the trimers. The bond distance reported in reference [10] agrees well with that obtained with ADF within 0.020 Å. As in the case of W_2, SIESTA predicts a shorter distance than the other methods.

Table 4. Atomization energies, E_{at} in eV/at, average bond lengths, R_{av} in Å, average coordination numbers, CN, and magnetic moments, μ in μ_B, for W_n clusters, with $n = 13$–23. See Figures 5 and 6 for labels.

Size	Method	E_{at}	R_{av}	CN	μ
13	SIESTA - *a*	5.11	2.614	5.23	0.15
	SIESTA - *b*	5.09	2.612	5.08	0.00
	ADF - *a*	5.31	2.669	5.23	0.00
	ADF - *b*	5.30	2.674	5.08	0.00
	Reference [10] - *a*	5.67	2.638	5.4	–
	Reference [10] - *b*	5.55	2.731	6.2	–
	Reference [10] - *c*	5.54	2.710	6.2	–
	Reference [10] - *d*	5.52	2.660	5.4	–
	Reference [10] - *e*	5.38	2.757	6.5	–
14	SIESTA - *a*	5.11	2.622	5.28	0.14
	SIESTA - *b*	5.11	2.635	5.43	0.00
	ADF - *a*	5.32	2.688	5.43	0.00
	ADF - *b*	5.32	2.689	5.43	0.14
	Reference [10] - *a*	5.73	2.706	6.3	–
	Reference [10] - *b*	5.72	2.702	6.0	–
	Reference [10] - *c*	5.71	2.699	6.7	–
15	SIESTA - *a*	5.17	2.643	5.47	0.13
	SIESTA - *b*	5.17	2.738	6.67	0.93
	ADF - *a*	5.37	2.707	5.60	0.13
	ADF - *b*	5.34	2.793	6.67	0.93
	Reference [10] - *a*	5.82	2.755	6.7	–
	Reference [10] - *b*	5.81	2.674	6.3	–
	Reference [10] - *c*	5.67	2.677	5.6	–
	Reference [10] - *d*	5.53	2.625	6.0	–
16	SIESTA - *a*	5.26	2.665	5.87	0.25
	SIESTA - *b*	5.21	2.738	6.62	0.25
	ADF - *a*	5.44	2.718	5.87	0.13
	ADF - *b*	5.40	2.790	6.75	0.13
	Reference [10] - *a*	5.83	2.716	6.3	–
	Reference [10] - *b*	5.77	2.648	5.5	–
	Reference [10] - *c*	5.76	2.681	5.8	–
19	SIESTA - *a*	5.37	2.691	6.32	0.00
	SIESTA - *b*	5.36	2.682	6.32	0.11
	ADF	5.56	2.738	6.32	0.00
23	SIESTA - *a*	5.50	2.728	6.69	0.09
	SIESTA - *b*	5.49	2.714	6.52	0.00
	ADF	5.67	2.755	6.52	0.17

For the tetramer, all programs predict a 3D geometry to be the ground state. Interestingly, an oblated tetrahedral geometry is reported for the ground state of W_4 in all cases. A singlet electronic state is found to be the ground electronic state according both to SIESTA and to ADF. Average bond distance is slightly larger in ADF than in SIESTA, and both, in turn, are larger than that reported in reference [10]. ADF predicts the second most stable tetramer to be a distorted tetrahedron, whereas a rhombic structure that slightly deviate from the planarity is predicted by SIESTA.

The lowest energy pentamer obtained with ADF is derived from the oblated tetrahedral found for W_4 and adopts a distorted trigonal bipyramidal geometry. The second lowest energy pentamer found by ADF grows from the distorted tetrahedron labeled 4-*b* by capping a W-W bond. The two lowest energy pentamers obtained with SIESTA present very similar geometries, which can be described as distorted trigonal bipyramids. They differ only in the electron multiplicity. Both programs predict the ground state of W_5 to be a triplet electronic state.

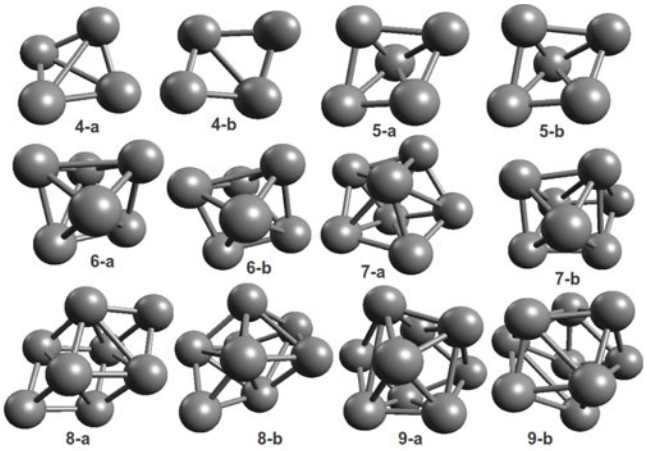

Fig. 1. Equilibrium geometries of W_n, $n = 4$–9, obtained with the SIESTA package. Labels correspond to those used in Tables 2 and 3.

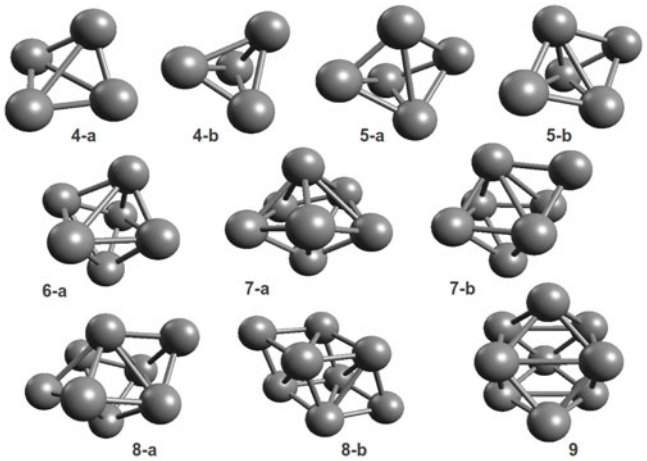

Fig. 2. Equilibrium geometries of W_n, $n = 4$–9, obtained with the ADF package. Labels correspond to those used in Tables 2 and 3.

The most stable hexamer obtained with SIESTA, 6-*a*, is derived from the distorted trigonal bipyramid geometries described above. The resulting geometry can be described as a strongly distorted octahedron. The second most stable hexamer, on the other hand, can be described as a slightly distorted octahedron. The lowest energy hexamer obtained with ADF becomes very similar to the most stable isomer found by SIESTA, described as a strongly distorted octahedron. In both cases, the ground state of W_6 is found to be a triplet electronic state.

The heptamer with the lowest energy obtained with SIESTA, 7-*a*, could be described as a distorted pentagonal bipyramid. Heptamer 7-*b* obtained with SIESTA is a derivative of hexamer 6-*b* in the sense that the seventh

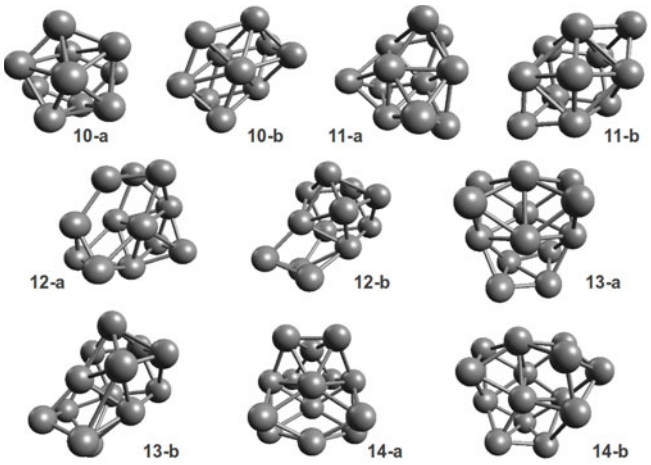

Fig. 3. Equilibrium geometries of W_n, $n = 10$–14, obtained with the SIESTA package. Labels correspond to those used in Tables 3 and 4.

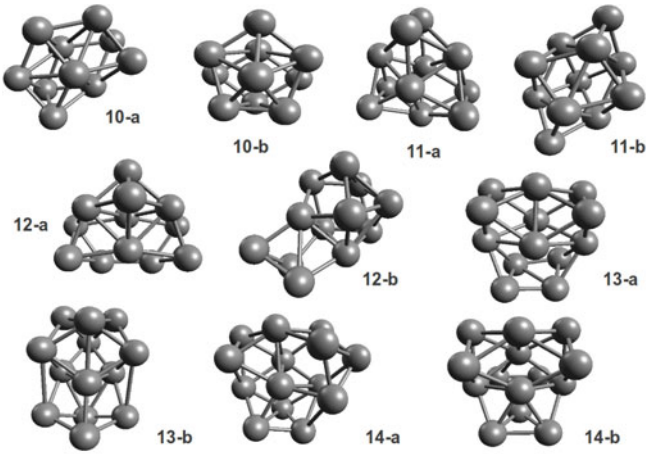

Fig. 4. Equilibrium geometries of W_n, $n = 10$–14, obtained with the ADF package. Labels correspond to those used in Tables 3 and 4.

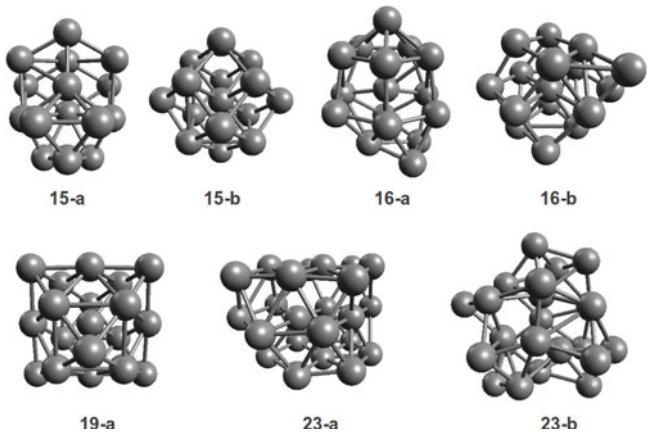

Fig. 5. Equilibrium geometries of W_n, $n = 15, 16, 19, 23$, obtained with the SIESTA package. Labels correspond to those used in Table 4. Isomer 19-*b* is not shown because it is very similar to 19-*a*.

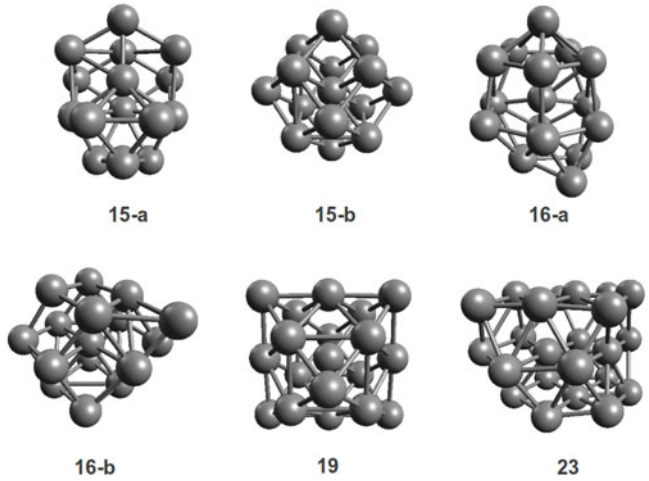

Fig. 6. Equilibrium geometries of W_n, $n = 15, 16, 19, 23$, obtained with the ADF package. Labels correspond to those used in Table 4.

tungsten atom caps a triangular face. The most stable heptamer obtained with ADF, 7-*a*, is also derived from the lowest energy hexamer after a triangular face is capped by the additional W atom. An important rearrangement occurs and the coordination number of the seventh tungsten atom increases from 3 to 4. The second most stable heptamer obtained with ADF is very similar to the 7-*b* structure obtained with SIESTA. It is derived from an slightly distorted octahedron by capping a triangular face. As in the case of SIESTA, the coordination number of the seventh W atom remains equal to 3. Both programs predict the ground state of W_7 to be a triplet electronic state.

The two lowest-energy octamers obtained with SIESTA are closely related to the heptamers discussed above. The most stable W_8 aggregate derives from the 7-*b* structure and it is characterized by a bicapped octahedron, in which the two capping atoms present a coordination number of 3. On the other hand, the second most stable octamer calculated with SIESTA, *b*, is clearly derived from the 7-*a* heptamer by capping a triangular face. The two lowest-energy octamers obtained with ADF are closely related to the geometries found with SIESTA. The 8-*a* aggregate is similar to the *b* species obtained with SIESTA, whereas the equilibrium geometry of 8-*b* agrees with the structure reported as 8-*a* by the SIESTA program. The most stable octamers calculated with ADF and with SIESTA are characterized by a triplet and by a quintet electronic state, respectively.

The only stable W_9 cluster obtained with ADF could be described as a strongly distorted square anti-prism in which a square face is capped by the additional W atom. The resulting geometry, however, is quite symmetric. This species is characterized by a singlet electronic state. The two stable W_9 aggregates calculated with SIESTA present the same equilibrium structure as can be seen from the average bond lengths reported in Table 3, see also Figure 1. They are represented by a mono-capped square antiprism. They differ, nevertheless, in the electronic state. The ground state presents a singlet electronic state.

The most stable W_{10} species obtained with SIESTA derives from the structures reported for W_9 after the additional W atom caps a rhombic face. The second most stable structure obtained with SIESTA for W_{10} could be described as two octahedra sharing a face and the additional atom capping a W-W bond. The most stable W_{10} isomer obtained with ADF agrees with structure 10-*b* found with SIESTA. On the other hand, the second most stable ADF structure is identical to the most stable geometry obtained with SIESTA. The ground state predicted by SIESTA is a septet electronic state, whereas ADF anticipates a doublet electronic state.

Two almost degenerate W_{11} species are found with SIESTA. The most stable one derives from 10-*b* and could be described as three distorted octahedra sharing three faces. 11-*b*, on the other hand, is a triangular prism, in which all its triangular and square faces have been mono-capped. The two most stable W_{11} structures found with ADF agree with isomers 11-*a* and 11-*b*, respectively, predicted by SIESTA. Nevertheless, the electronic state of the ground state found with SIESTA is a singlet, whereas a triplet electronic state characterizes the ground state predicted by ADF.

As in the previous case, SIESTA predicts two almost degenerate W_{12} aggregates. Structure 12-*a* derives from 11-*a* after the new atom caps a triangular face. Moreover, an important rearrangement occurs and the mono-capped triangular face no longer exists when 12-*a* reaches its equilibrium geometry. The second most stable W_{12} cluster derives from 10-*a* or even from 9-*a* rather than from the more symmetric 11-*b* structure. It could be described as the addition of a W_3 unit to a triangular face of the structure reported as 9-*a* by SIESTA. In this case, ADF yields two almost degenerate aggregates, too. The most stable structure obtained with ADF agrees with isomer 12-*a* predicted by SIESTA. On the other hand, the geometry of structure 12-*b* predicted by ADF becomes identical to the 12-*b* cluster obtained with SIESTA. Interestingly, the ground state predicted by the two programs is a singlet electronic state.

The most stable W_{13} structure obtained with SIESTA grows from isomer 12-*a* after a rhombic face is mono-capped by the additional atom. Interestingly, structure 13-*b* could be characterized as a derivative of 12-*b*, in which a rhombic face becomes mono-capped by the new atom. The two most stable structures obtained with ADF are related to the ones achieved with SIESTA. The most stable one agrees with geometry 13-*a* from SIESTA, whereas the second most stable aggregate obtained with ADF becomes identical to isomer 13-*b* from SIESTA. The multiplicities of the ground state are differently described by the two programs. ADF predicts a singlet electronic state and SIESTA leads to a triplet electronic state.

The two most stable W_{14} structures achieved with SIESTA are almost degenerate as can be observed from the atomization energies reported in Table 4. The most stable structure, 14-*a*, is formed after a rhombic face of 13-*a* is mono-capped by the additional atom, resulting in a more symmetric geometry than the original one. The second most stable geometry, 14-*b*, is also derived from 13-*a* after a rhombic face becomes mono-capped by the new atom. In this later case, however, a rearrangement takes place leading to an important distortion of the original geometry. The two most stable W_{14} structures obtained with ADF are very close in energy, differing only in 0.008 eV/at, see Table 4. Interestingly, those geometries are related to the ones obtained with SIESTA, too. Isomers 14-*a* and 14-*b* achieved with ADF agree with SIESTA structures 14-*b* and 14-*a*, respectively. The ground state predicted by ADF is a singlet electronic state, whereas a triplet electronic state characterizes the ground state of W_{14} according SIESTA.

The SIESTA program predicts two almost degenerate structures as the most stable species for W_{15}. The most stable structure, 15-*a*, is formed from 14-*a* after a rhombic face is mono-capped by the additional atom. It is very important to note that structure 15-*b* exhibits a perfect body-centered cubic geometry, indicating a change in the way small tungsten clusters grow. The most stable W_{15} aggregates obtained with ADF follow a similar growing pattern that the one observed for SIESTA. Structures 15-*a* and 15-*b* are the same as SIESTA geometries 15-*a* and 15-*b*, respectively. Furthermore, the two programs agree to predict that the most stable structures present a triplet electronic ground state, whereas the *bcc* geometries exhibit an electronic spin multiplicity of 14. These results are relevant considering the suggestion made in references [4,5] that a change in the chemical reactivity features of tungsten aggregates up to 60 atoms is observed at a size of 15 atoms and, moreover, it could be attributed to a structural transition.

The most stable W_{16} structure obtained with SIESTA is formed by two pentagonal bi-pyramids, which share an atom. The three additional W atoms cap triangular faces of only one of the bi-pyramids producing an important distortion that makes it difficult to identify the equilibrium geometry. The second most stable structure, 16-*b*, derives from 15-*b* after a rhombic face becomes mono-capped by the additional atom. A slightly distorted *bcc* structure is obtained. The two most stable W_{16} species achieved with ADF exhibit the same equilibrium geometries that the ones obtained with SIESTA, see Figures 5 and 6. The ground state of W_{16} is predicted to be a quintet electronic state by SIESTA, whereas ADF delivers a triplet electronic state.

The two most stable W_{19} structures found with SIESTA are derivatives of the *bcc* system, see Figure 5. Both aggregates are rather similar and are distorted with respect to a perfect *bcc* cluster containing 19 atoms. They present, however, different electron multiplicities. ADF predicts only one stable W_{19} isomer, see Figure 6, which, in turn, also derives from the *bcc* system. A singlet electronic state is found to characterize the ground state of W_{19} according to the two programs used in the present work.

The two most stable W_{23} structures found with SIESTA are depicted in Figure 5. Structure 23-*a* is a rather distorted version of a portion of a hexagonal close-packed system consisting of two parallel and adjacent 8-atom

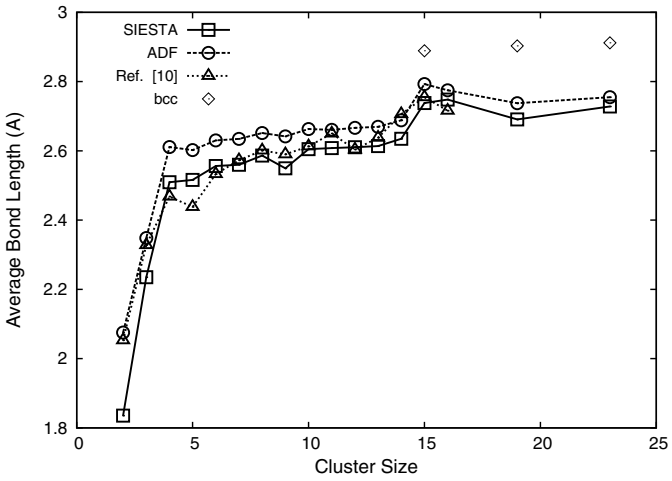

Fig. 7. Average bond lenghts, in Å, as a function of cluster size. Results obtained with SIESTA and ADF are shown and compared with those reported in reference [10]. Average bond lengths for *bcc* aggregates with 15, 19 and 23 atoms are also shown. For those cases in which degeneracy or cuasi-degeneracy is observed, the larger average bond length is used in the figure.

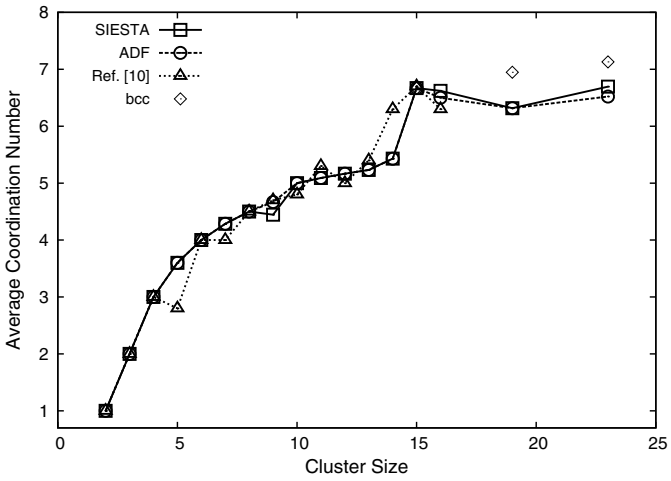

Fig. 8. Average coordination numbers as a function of cluster size. Results obtained with SIESTA and ADF are shown and compared with those reported in reference [10]. Average coordination numbers for *bcc* aggregates with 15, 19 and 23 atoms are also shown. For those cases in which degeneracy or cuasi-degeneracy is observed, the larger coordination number is used in the figure.

planes and a third plane having 7 atoms. Isomer 23-*b*, on the other hand, presents a strongly distorted geometry derived from a poly-icosahedral structure. As in the previous case of 19 atoms, only one W_{23} structure is found with ADF. It agrees with the 23-*a* structure found with SIESTA. The ground state of W_{23} is found to be a triplet electronic state and a quintet electronic state according to SIESTA and ADF, respectively.

A careful comparison of the equilibrium geometries obtained in the present work with those reported in reference [10] shows that the agreement between the different approximations to the DFT is very good up to $n = 9$, SIESTA and ADF exhibiting more distorted structures, though. For $n = 10$, the most stable structure found with ADF agrees well with the one reported in reference [10], but the ground state found with SIESTA is in line with a higher energy isomer described in reference [10]. There is a good agreement between the geometries obtained with ADF and SIESTA for sizes from $n = 11$ to $n = 14$. Those structures differ largely from the equilibrium geometries shown in reference [10], being in general less symmetric. For sizes with $n = 15$ and above a general agreement is observed again between the three approximations to the DFT, mainly because the most stable isomers derive from the *bcc* system.

Figure 7 shows the dependence of the average bond length on the cluster size. It is observed that results achieved with ADF and SIESTA tend smoothly to the bulk limit of 3.16 Å, whereas results reported in reference [10] exhibit a more erratic behavior. The corresponding values for perfect *bcc* structures containing 15, 19 and 23 atoms, also shown in the figure, present the same tendency with higher initial values.

Figure 8 shows the variation of the average coordination number with the cluster size obtained with ADF and SIESTA. A smooth increase in the coordination number is observed up to $n = 14$ for results achieved both with SIESTA and ADF and for results reported in reference [10]. A jump is seen in the figure for the three approximations to the DFT when $n = 15$, indicating that a change in the growing pattern of the aggregates takes place. The departure from values for perfect *bcc* structures for larger cluster sizes is mainly due to distortions in the equilibrium geometries. As indicated above, these results are relevant concerning the suggestion that the change in the chemical reactivity of small tungsten aggregates at a size of 15 atoms could be attributed to a structural transition from closed-packed structures to open structures [4,5]. However, it should be noted that present results suggest that the transition about $n = 15$ occurs from open structures to more closed geometries with a *bcc* pattern. These facts are very interesting and deserve further investigation of chemical reactivity of W_n clusters around $n = 15$ with molecular nitrogen from a computational point of view.

3.2 Electronic and magnetic properties of W_n clusters

Figure 9 shows the second-order total energy difference as a function of the cluster size. It can be seen from the figure that the BPW91 approximation to the DFT predicts three cluster sizes to be more stable relative to their neighbors. They are W_8, W_{12} and W_{15} [10]. It can also be observed in the figure that both the PBE (SIESTA) and BLYP (ADF) approximations to DFT agree to characterize W_8 as a very stable aggregate with respect to its neighbors. Nevertheless, W_{12} is described as the less stable cluster with respect to its neighbors in the present study. A consequence of this is that both W_{11} and W_{13} are extremely stable with respect to their neighbors according to results obtained with ADF. W_{13} is also found to be very stable

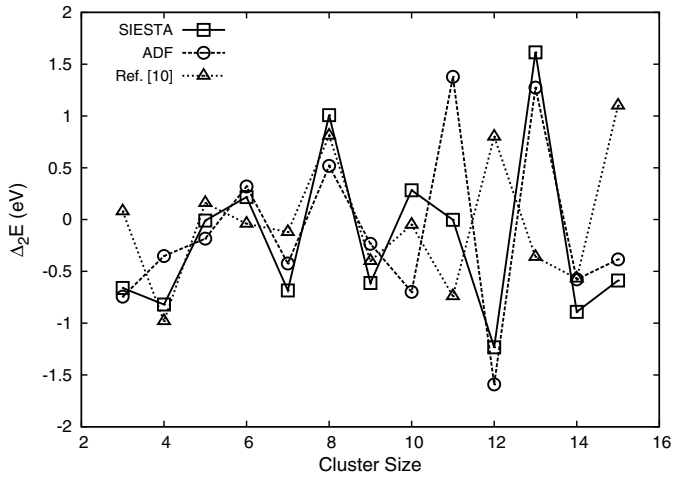

Fig. 9. Second-order total energy differences, in eV, as a function of cluster size. Results obtained with SIESTA and ADF are shown and compared with those reported in reference [10].

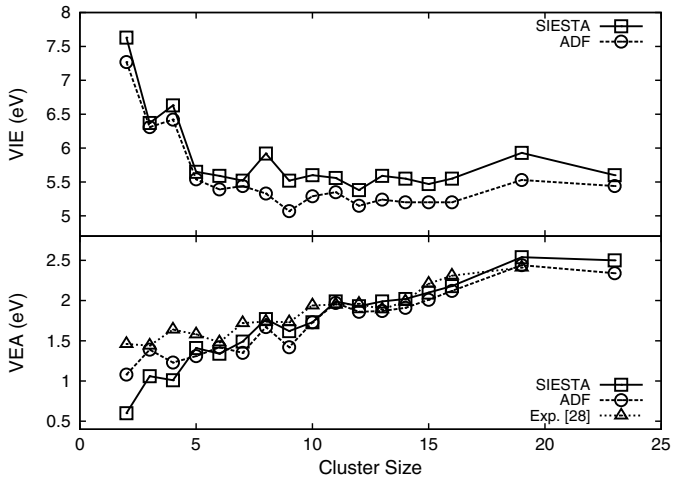

Fig. 10. Vertical ionization energies and vertical electron affinities, in eV, as a function of cluster size. Results obtained with SIESTA and ADF are shown and compared with experimental vertical electron detachment energies reported in reference [28].

with respect to its neighbors according to the SIESTA program, but nothing special is appreciated for W_{11}. Then, it is very interesting to note that even though different GGA approximations to the DFT could deliver similar geometries for the most stable tungsten clusters, they could show very different relative stability patterns.

Figure 10 shows the variation of VIE and VEA as a function of the cluster size. VIE's exhibit a steep descent from $n = 2$ up to $n = 5$. Then, VIE's show a slight variation around a value of about 5.4 eV, which is distant from the value of 4.55 eV, the experimental work function of tungsten [29]. VEA's, on the other hand, show a smooth increase up to values about 2.4 eV for the larger sizes studied in the present work. The agreement with experimental values of electron detachment energies [28] is very remarkable.

Finally, the magnetic moments listed in Tables 2 to 4 show that electronic states of the most stable W_n isomer for every size are singlet, triplet or quintet states. The only exception is W_{10}, for which the most stable isomer calculated with SIESTA presents a septet electronic state. It is also worth mentioning that the second most stable W_{15} species, calculated both with SIESTA and with ADF as a perfect portion of the *bcc* system, presents 14 unpaired electrons. Although more calculations are required, the presence of 14 unpaired electrons could convert the *bcc* W_{15} aggregate in a highly reactive species, explaining partially the change in the reactivity pattern observed experimentally [4,5]. It is also important to mention that, as expected, the total energy curve with respect to the electron multiplicity becomes more shallow as the size of the cluster increases and, then, various low-laying isomers with higher electron multiplicities should be available at room temperature experiments.

4 Conclusions

The geometrical, electronic and magnetic properties of small tungsten clusters with 2-16, 19 and 23 atoms were studied with different approximations to the density functional theory as implemented in two different programs. Moreover, present results are compared with others achieved with a third approximation to the density functional theory as coded in another program. Basis sets were of similar quality.

It is found that equilibrium geometries of the most stable isomers found for every size studied are very similar irrespective of the approximation to the density functional theory used.

The inspection of equilibrium geometries allowed to detect that for sizes with 15 atoms and above, aggregates with a structure derived from the body-centered cubic systems are preferred, indicating a transition from open structures to more closed geometries. Nevertheless, body-centered cubic structures are not perfect as can be deduced from average coordination numbers.

The relative stability of aggregates with respect to their neighbors predicted the octamer to be specially stable by the three programs under comparison. However, there are discrepancies in the relative stability of clusters having 11 to 15 atoms.

Electronic states of most stable isomers were found to be singlets, triplets or quintets in the majority of the cases studied. An aggregate with 15 atoms and a body-centered cubic structure was found to have 14 unpaired electrons, a fact that could indicate an important chemical reactivity.

Calculated vertical ionization energies shown a very smooth tendency to the experimental work function of polycrystalline tungsten. Calculated vertical electron affinities describe very well experimental values of vertical electron detachment energies of small tungsten clusters.

The authors acknowledge CONICET and ANPCyT (Argentina), CONACyT (Mexico) and Ministerio de Educación, Cultura y Deporte (Spain) for financial support. S.M.C.

is a research fellow from ANPCyT. R.P.D. is member of the Scientific Research Career of CONICET. F.A.-G. acknowledges financial support from SEP-PROMEP CA230, CONACyT 162651 and Ministerio de Educación, Cultura y Deporte, Ref. SAB2011-0024, Spain.

References

1. C.H. Kline, V. Kollonitsch, Ind. Eng. Chem. **57**, 53 (1965)
2. *Theory of Atomic and Molecular Clusters*, edited by J. Jellinek (Springer, Berlin, 1999)
3. R.L. Johnston, *Atomic and Molecular Clusters* (Taylor and Francis, London, 2002)
4. S.A. Mitchell, D.M. Rayner, T. Bartlett, P.A. Hackett, J. Chem. Phys. **104**, 4012 (1996)
5. L. Holmgren, M. Andersson, A. Rosén, J. Chem. Phys. **109**, 3232 (1998)
6. Y.D. Kim, D. Stolcic, M. Fischer, G. Ganteför, J. Chem. Phys. **119**, 10307 (2003)
7. Z.J. Wu, Chem. Phys. Lett. **370**, 510 (2003)
8. X.R. Zhang, X.L. Ding, B. Dai, J.L. Yang, J. Mol. Struct.: THEOCHEM **757**, 113 (2005)
9. W. Yamaguchi, J. Murakami, Chem. Phys. **316**, 45 (2005)
10. J. Du, X. Sun, D. Meng, P. Zhang, G. Jiang, J. Chem. Phys. **131**, 044313 (2009)
11. P. Hohenberg, W. Kohn, Phys. Rev. **136**, B864 (1964)
12. W. Kohn, L.J. Sham, Phys. Rev. **140**, A1133 (1965)
13. R.G. Parr, W. Yang, *Density Functional Theory of Atoms and Molecules* (Oxford University Press, 1989)
14. J.M. Soler, E. Artacho, J.D. Gale, A. García, J. Junquera, P. Ordejon, D. Sánchez-Portal, J. Phys.: Condens. Matter **14**, 2745 (2002)
15. J.P. Perdew, K. Burke, M. Ernzerhof, Phys. Rev. Lett. **77**, 3865 (1996)
16. N. Troullier, J.L. Martins, Phys. Rev. B **43**, 1993 (1991)
17. L. Kleinman, D.M. Bylander, Phys. Rev. Lett. **48**, 1425 (1982)
18. ADF2010, SCM, Theoretical Chemistry, Vrije Universiteit, Amsterdam, The Netherlands, http://www.scm.com
19. C.F. Guerra, J.G. Snijders, G. Te Velde, E.J. Baerends, Theor. Chem. Acc. **99**, 391 (1998)
20. G. Te Velde, F.M. Bickelhaupt, S.J.A. Van Gisbergen, C.F. Guerra, E.J. Baerends, J.G. Snijders, T. Ziegler, J. Comput. Chem. **22**, 931 (2001)
21. A.D. Becke, Phys. Rev. A **38**, 3098 (1988)
22. C. Lee, W. Yang, R.G. Parr, Phys. Rev. B **37**, 785 (1988)
23. E. van Lenthe, E.J. Baerends, J.G. Snijders, J. Chem. Phys. **99**, 4597 (1993)
24. E. van Lenthe, E.J. Baerends, J.G. Snijders, J. Chem. Phys. **101**, 9783 (1994)
25. E. van Lenthe, A.E. Ehlers, E.J. Baerends, J. Chem. Phys. **110**, 8943 (1999)
26. J.E. Sansonetti, W.C. Martin, J. Phys. Chem. Ref. Data **34**, 1559 (2005)
27. C. Angeli, A. Cavallini, R. Cimiraglia, J. Chem. Phys. **127**, 074306 (2007)
28. H. Weidele, D. Kreisle, E. Recknagel, G.S. Icking-Konert, H. Handschuh, G. Ganteför, W. Eberhardt, Chem. Phys. Lett. **237**, 425 (1995)
29. H.B. Michaelson, J. Appl. Phys. **48**, 4729 (1977)